www.czasopisma.pan.pl PAN POLSKA AKADEMIA NAUK www.journals.pan.pl

A R C H I V E S O F M E T A L L U R G Y A N D M A T E R I A L S

Volume 58 2013 Issue 4

DOI: 10.2478/amm-2013-0138

V.V. ÇAY*, S. OZAN**, M.S. GÖK***, A. ERDOĞAN****

THE EFFECT OF SHIELDING GAS COMPOSITION ON MICROSTRUCTURE AND ABRASIVE WEAR RESISTANCE FABRICATED WITH PTA ALLOYING TECHNIQUE

WPŁYW SKŁADU GAZU OSŁONOWEGO NA MIKROSTRUKTURĘ I ODPORNOŚĆ NA ŚCIERANIE POWŁOK WYTWORZONYCH TECHNIKĄ PTA

In this study, SAE 1020 steel surfaces were separately alloyed with preplaced high-carbon-ferro-chromium (FeCr), ferro-molybdenum (FeMo) and ferro-titanium (FeTi) powders by using plasma transferred arc (PTA) heat source. By using three different types of shielding gas compositions during the alloying process, the study investigated the effects of modified shielding gas composition on the microstructure, hardness, and abrasive wear resistance of specimens. The most homogenous microstructure and the highest wear resistance was obtained in the gaseous environment which included 3% of H_2. Increasing this rate to 5 % in the shielding gaseous composition caused gaps and pores in the microstructure and caused a decrease in the wear resistance. The x-ray examinations of the specimens identified ferro-molybdenum and ferro-titanium solid solutions, ferrit, austenite and martensite phases in their microstructure as the first phase and FeC, Cr_7C_3, Cr_3C_2, Fe_3C, Fe_7C_3, MoC and TiC phases as the second phase. As a result, it was concluded that changes in shielding gas composition in surface alloying process affected specimens' microstructure and abrasive wear properties.

Keywords: Surface modification, shielding gas, PTA, alloying, microstructure

Powierzchnie stalowe SAE 1020 były oddzielnie stopowane z wcześniej nałożonymi proszkami wysokowęglowego żelazo-chromu (FeCr), żelazo-molibdenu (FeMo) i żelazo-tytanu (FeTi) za pomocą techniki PTA. Dzięki zastosowaniu trzech różnych typów gazu osłonowego w trakcie procesu wytwarzania stopu, badano wpływ modyfikacji składu gazu osłonowego na mikrostrukturę, twardość i odporność na ścieranie próbek. Najbardziej jednorodną mikrostrukturę i najwyższą odporność na ścieranie otrzymuje się w środowisku gazowym, które zawiera 3% H_2. Zwiększenie zawartości H_2 do 5% w składzie gazu osłonowego spowodowało powstanie luk i porów w mikrostrukturze oraz spadek odporności na ścieranie. Badania dyfrakcji rentgenowskiej próbek pozwoliły zidentyfikować roztwory stałe żelazo-molibdenu i żelazo-tytanu, ferryt, austenit i martenzyt jako pierwszą fazę w ich mikrostrukturze, oraz FeC, Cr_7C_3, Cr_3C_2, Fe_3C, Fe_7C_3, MoC i TiC jako drugą fazę. W związku z tym stwierdzono, że zmiany w składu gazu osłonowego w procesie stopowania wpłynęły na mikrostrukturę próbek i właściwości ścierne.

1. Introduction

For moving metallic mechanical components wear is the most common failure mode. Wear can also be defined as a problem results in loss of material from surfaces where interaction between two surfaces [1]. The use of surface engineering enable forming microstructure, chemical composition and state of internal stresses [2]. From both economic and technological points, producing a coating which has a high-performance wear-resistant on the surface of tribological components with appropriate surface engineering technology is one of the most efficient approaches to enhance the tribological performance for many moving mechanical components. Between the widely used surface engineering technologies, laser cladding, plasma transferred arc (PTA) weldsurfacing, flame spray and plasma spray can fabricate a relative thicker coating [3-12].

In arc welding, the composition of a shielding mixture connects generally to the kind of material to be welded. The determination of the shielding gas should consider chemical–metallurgical processes between the gases and the molten pool that occur during welding [13]. Hydrogen is prone to turbulent flow at the exit from the blowpipe nozzle due to thermal buoyancy also hydrogen is 10 and 20 times less dense than argon. Argon gas density is 1.669 kg/m^3, whereas density of hydrogen in 15°C is 0.085 kg/m^3 [14].

Hydrogen as a shielding gas is used as an addition to argon, helium and nitrogen [15]. The addition of hydrogen also significantly increases the volume of molten material in the weld pool due to the higher thermal conductivity of

* VOCATIONAL SCHOOL OF HIGHER EDUCATION, DICLE UNIVERSITY, DIYARBAKIR, TURKEY
** DEPARTMENT OF METALLURGY, FACULTY OF TECHNICAL EDUCATION, UNIVERSITY OF FIRAT, ELAZIG TURKEY
*** DEPARTMENT OF METALLURGICAL ENGINEERING, FACULTY OF ENGINEERING, BARTIN UNIVERSITY, BARTIN, TURKEY
**** DEPARTMENT OF METALLURGICAL ENGINEERING, FACULTY OF ENGINEERING, BARTIN UNIVERSITY, BARTIN, TURKEY

argon-hydrogen mixtures at temperatures at which molecules of hydrogen dissociate [16-17]. In the welding of high-alloy stainless steels hydrogen has only lately been added to argon. In TIG and MIG welding applications an argon–hydrogen mixture may be used [14]. The argon-hydrogen mixture has been recently increasingly used as a shielding gas in arc welding of austenitic stainless steels, ferritic and martensitic steels. The majority of the authors who studies on shielded-gas welding recommends 0.5%-5% hydrogen in argon. Hydrogen prevents the oxide formation on the surface of the layer of the weld. Weld appearance is therefore nicer. On the other hand the addition of hydrogen to a shielding atmosphere may create some difficulties. Hydrogen solubility in molten metals is very high. Therefore in steels and other metals hydrogen may produce gas bubbles and cracks [13].

Both TIG (Tungsten Inert Gas) and PTA (plasma transferred arc) methods are employed in surface modification applications [18-20]. In previous study which was implemented by using the TIG method, the effects of two different types of shielding gas on welding pool was investigated [21]. In this study, three different types of shielding gas were used and surface modification was applied with PTA method. The present study investigated the effects of changes in shielding gas composition on the microstructure and abrasive wear characteristics of coatings in specimens surface-alloyed with FeCr, FeMo and FeTi.

2. Experimental

High-carbon-ferro-chromium, ferro-molybdenum and ferro-titanium coatings were carried out on low carbon steel (SAE 1020) plate by using plasma transferred (PTA) arc. The operating principle of PTA melting used was schematically shown in Fig. 1.

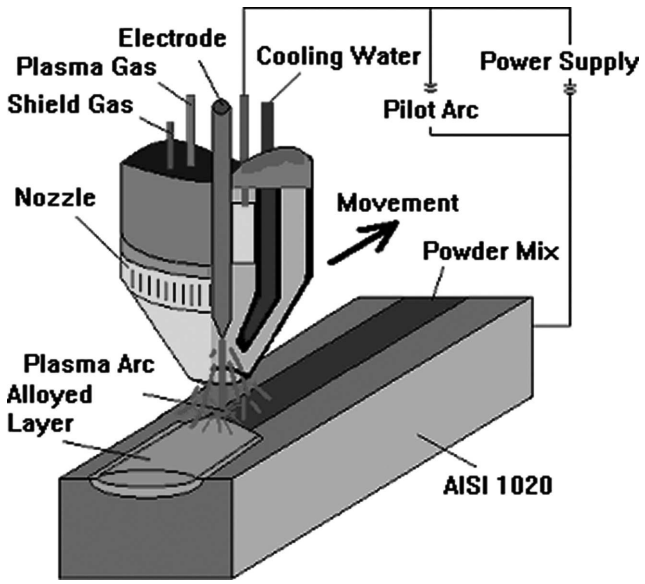

Fig. 1. Process diagram of plasma transferred arc welding

Surface coating procedure was realized 80 amperes welding currents and three different shielding gas composition. Parameters of the PTA deposition were given in Table 1.

TABLE 1

PTA experimental parameters

Arc current (A)	80
Energy input (kj/mm)	0.65
Arc voltage (V)	18
Shield gas flow (Ar,Ar+H_2, l/min)	25
Plasma gas flow (Ar, l/min)	0.8
Diameter of electrode (mm)	4.7
Travel speed (mm/s)	2.2
Torch gap (mm)	3

Low carbon steel plates of 100×20×10 mm in dimension were cut and then polished down to 1200 grit abrasive paper and finally rinsed with ethyl alcohol before coating. The powders mixed with sodium silicate were then drayed in hot air to obtain regular surface deposition and not to scatter around the powders on the surface under the pressure of shielding gas during arc-melting. A groove, 1.5 mm in depth and 10 mm in width, machined on the surface of the substrate by a milling machine and mixed powders were applied into this groove and dried in hot air. Chemical compositions of substrate and coating material were presented in Table 2. Plasma arc was used as the heat source to melt the coating layer and substrate.

TABLE 2

Chemical compositions (wt. %) of welding specimen and powders for surface alloying

	C	Si	Mn	P	S	Cr	Ti	Mo	Fe
SAE 1020	0.185	0.281	0.518	0.024	0.034	-	-	-	Balance
FeCr	7.65	0.65	-	0.016	0.050	67.18		-	Balance
FeMo	0.15	1.56	-	0.05	0.15	-	-	68	Balance
FeTi	1.25	1,19	-	0.025	0.031	-	73.45	-	Balance

Following surface alloying, the samples were cut from the alloyed specimens for micro-structural examination and hardness measurements. The samples were prepared for metallographic examination by grinding on SiC wheels followed by polishing. The microstructure of the samples was etched by a solution containing 5 ml HNO_3 200 ml HCl 65 gr $FeCl_2$. Conventional characterization techniques, such as scanning electron microscopy (SEM), energy dispersive spectrograph (EDS) and X-ray diffraction were employed to study the microstructure and elemental analysis of the alloyed zone. The wear resistances of the alloyed surfaces were determined at room temperature by a two body pin-on-disc wear tester. Abrasive wear tests were performed on samples with the dimensions of 10×10×10 mm, impinging vertically on a rotating disc coated with the 80 mesh SiC. The wear specimen moved in a spiral path on the disc so that the specimen always moved over fresh abrasive. The abrasive papers were changed after each use. A load of 10-30 N was applied to the specimens. The frictional distance of a wear specimen on the disc was 20 m.

TABLE 3

Welding and process parameters

Specimen number	Coating Powder	Thickness Coating-mm	Energy Intensity	Hardness (HRc)	Shielding Gas Composition	Shielding Gas label
1	FeCr	1.50	80 A	64	Argon	P_1
2	FeCr	1.50	80 A	58	Argon+ 3 % H_2	P_2
3	FeCr	1.50	80 A	56	Argon+ 5 % H_2	P_3
4	FeMo	1.50	80 A	51	Argon	P_1
5	FeMo	1.50	80 A	53	Argon+ 3 % H_2	P_2
6	FeMo	1.50	80 A	44	Argon+ 5 % H_2	P_3
7	FeTi	1.50	80 A	40	Argon	P_1
8	FeTi	1.50	80 A	45	Argon+ 3 % H_2	P_2
9	FeTi	1.50	80 A	38	Argon+ 5 % H_2	P_3

3. Results and Discussion

3.1. Composition and microstructure of the alloyed zone

In this study, FeCr, FeMo and FeTi powders were alloyed on the surface of AISI 1020 steel using the PTA welding method. Three different types of shielding gas mixtures were used in the alloying process. Shielding gas compositions of the samples used in the surface modification operation was given in Table 3.

These compositions were labelled with short letters in (P_1-P_3) order to provide convenience within the text. Microstructure of the specimen 1 which was subject to surface modification by using FeCr powder in P_1 composition was given in Fig. 2a-b.

It was observed that the plate type of the microstructure was made of martensite and retained austenite. In P_2 and P_3 compositions, it was observed that the microstructure changes after the alloying operation performed by using FeCr powders. It was observed in both P_2 and P_3 compositions that the microstructure forms as carbide eutectic between dendrites Fig. 3.

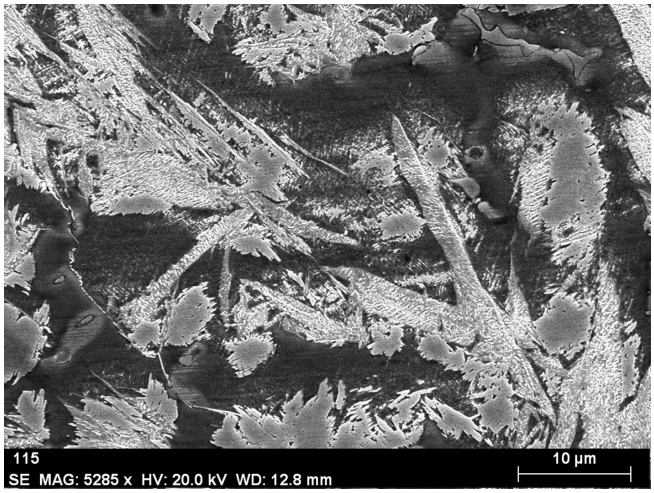

Fig. 2. a. SEM micrograph of the alloyed zone microstructure of specimen alloyed with FeCr powder (pure argon)
b. SEM micrograph of the alloyed zone microstructure of specimen alloyed with FeCr powder (pure argon)

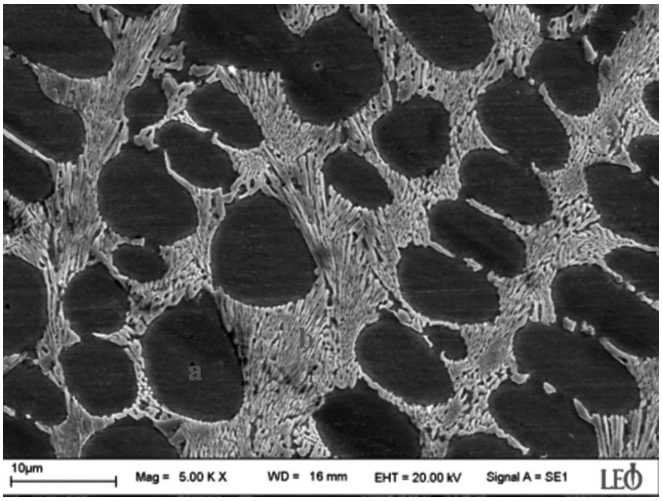

Fig. 3. SEM micrograph of the alloyed zone microstructure of specimen alloyed with FeCr powder (pure argon+ 3% H_2 gas)

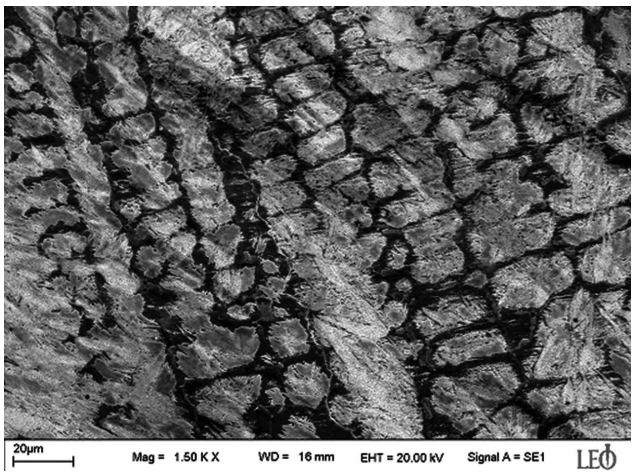

However, it was seen in the modification applied in P_2 composition that the dendrites are finer. The reason of this can

be linked to the difference in the cooling rates of the samples depending on the rates of the shielding gas as will be explained below. It is possible to associate the fact that the structure is martensite in P_1 composition with the feature of argon gas, because argon gas has lower heat conduction compared to hydrogen gas. Consequently, the lower energy input occurring in the sample welding pool causes the sample to cool faster. Therefore, it allowed the martensite phase to obtained. The reason of the change occurring in the microstructures due to the change in shielding gas composition can be associated to H_2 gas. Physical-chemical properties of each of the two gases are very different. Hydrogen gas enthalpy is higher than that of argon almost in the entire temperature range. Enthalpy of a shielding gas affects arc formation, arc shape, and temperature distribution in the arc as well. For the thermal conductivity of H_2 gas can increase tenfold depending on heat, while the thermal conductivity of argon gas is very low. Addition hydrogen addition to argon increases voltage drop in the arc, and consequently arc power due to high thermal conductivity of hydrogen. The arc gets narrower and energy concentration in it increases, which entails a deeper penetration. The effect of melting increases with increasing H_2 gas rate in shielding argon gas used in the PTA welding method [11-12].

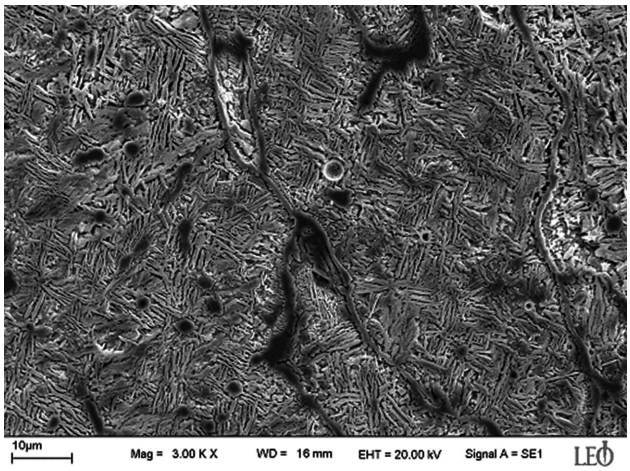

Fig. 4. SEM micrograph of the alloyed zone microstructure of specimen alloyed with FeMo powder (pure argon)

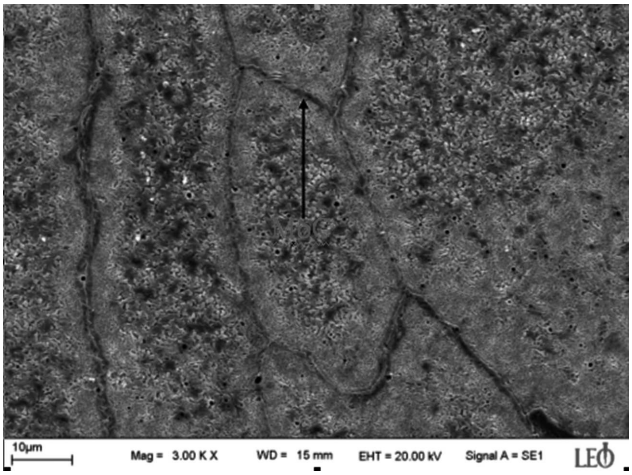

Fig. 5. SEM micrograph of the alloyed zone microstructure of specimen alloyed with FeMo powder (pure argon+ 3% H_2 gas)

The microstructure of the specimen 4 which was exposed to surface modification operation by using FeMo powders in P_1 composition is given in Fig. 4. The microstructure was formed as a eutectic of ferrite and molybdenum. Microstructure photograph of the Specimen 5 which was exposed to surface modification operation in P_2 composition is given in Fig. 5.

It was observed that the sample demonstrated a more homogeneous and fine microstructure after the operation. It was also observed that MoC phase which is rich in the element Mo settled in the boundry of grain. Since the other processes were kept fixed during the surface modification, it would be correct to evaluate this change in the microstructure with shielding gas composition. It was found by Tusek and Suban [11-12] also reported that the melting efficiency of TIG welding increases with increasing current intensity and hydrogen content in argon hydrogen, even with the same welding current, welding under shielding media, which contain hydrogen, causes more heat input into the welding zone. Adding H_2 to argon protective gas changes the static characteristic of welding arc and increases the fusing efficiency in the welding bath. A similar case was also observed after the operation performed by using the PTA method. With the effect of hydrogen in the welding pool, a more intense energy input occurs and the coating material obtains a more homogeneous and fine-grained structure. The carbide phase, which is formed as strips and places in the grain boundary, supports the adequate heat formation. It was observed that the surface modification performed in P_3 composition causes gaps or cracks and porosity in the microstructure of the sample (Fig. 6a-b).

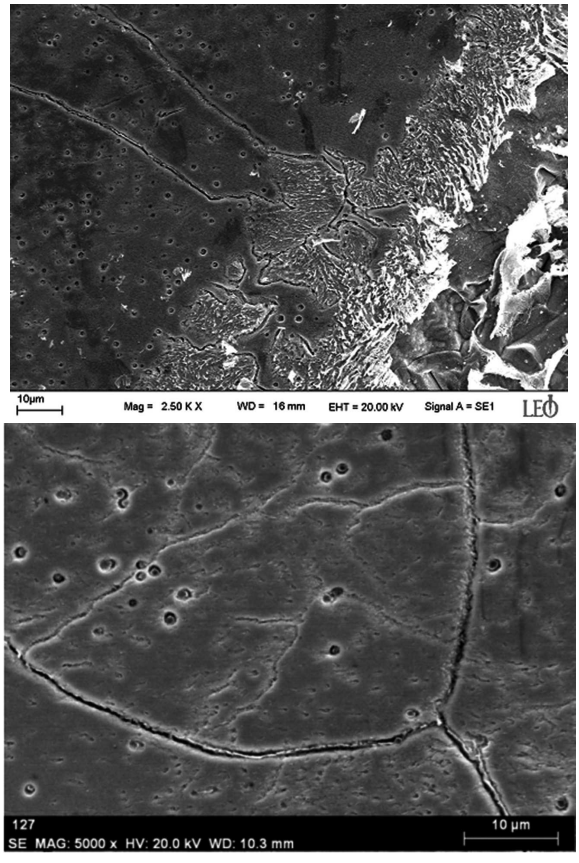

Fig. 6. SEM micrograph of the alloyed zone microstructure of specimen alloyed with FeMo powder (pure argon+5% H_2gas)

It was also seen that the cracks occurred between the MoC phase which places in the grain boundry and FeMo solid solution which constitutes the matrix. The porous structure occurred in the FeMo solid melt matrix, because H_2 which is trapped in higher amounts in the welding bath could not have the time to leave the environment.

Figure 7 shows the SEM microstructure photograph of the coating of specimen 7 following surface alloying using FeTi powder in P_1 gas composition. As is clear from the microstructure photograph, titanium element was not allowed a homogeneous distribution in the main mass and thus, some areas were rich in titanium content, while some remained as poor of titanium and rich of iron solid solution (ferrite).

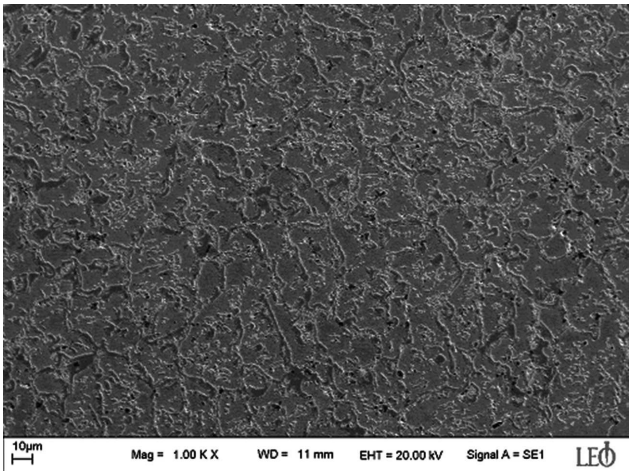

Fig. 7. SEM micrograph of the alloyed zone microstructure of specimen alloyed with FeTi powder (pure argon)

This could be attributed to insufficient heat in the welding pool and therefore, insufficient energy input. These can be related with the fact that operating current is low and also explained with the fact that argon gas has lower enthalpy and thermal conductivity compared to hydrogen. Following the surface modification process by changing the shielding gas composition P_2, it was observed that the microstructure of specimen 8 changed (Fig. 8).

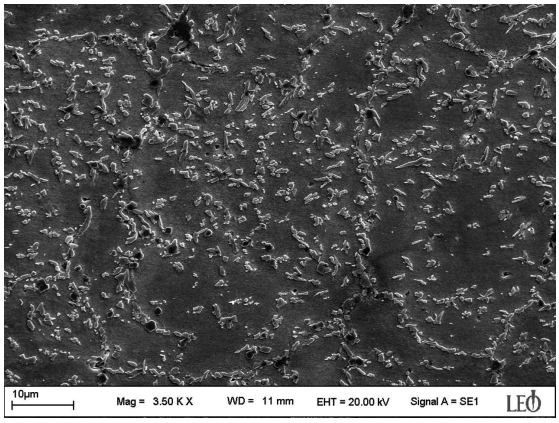

Fig. 8. SEM micrograph of the alloyed zone microstructure of specimen alloyed with FeTi powder (pure argon+ 3% H_2 gas)

The microstructure of the specimen reveals two different phases. The first is the main phase that dominates the microstructure and the other is the phase that forms in the first phase in the form of cells, and rods. Change in the microstructure could be attributed to the addition of hydrogen into argon shielding gas because hydrogen influences the static characteristics of welding current [11-12]. Hydrogen addition to argon increases voltage drop in the arc, and consequently arc power. Due to high thermal conductivity of hydrogen, the arc gets narrower and energy concentration in it increases, which entails a deeper penetration [12]. Thus, as a result of sufficient and high temperature in the welding bath due to high energy supply, titanium and carbon elements reached a higher diffusion speed and with slower cooling process TiC was formed in the microstructure. It was observed in the sample performed in the P_3 protective gas composition that micro spaces formed between phases as in the specimen 9. The influence of external hydrogen would be affected by the adsorption of surface hydrogen and thetransportation of hydrogen to the embrittled region see Fig. 9.

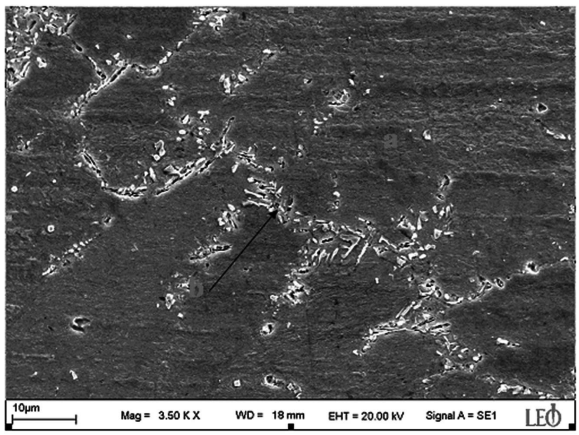

Fig. 9. SEM micrograph of the alloyed zone microstructure of specimen alloyed with FeTi powder (pure argon+ 5% H_2 gas)

XRD spectra were performed in order to determine the phases occurring in the samples. Moreover, EDS analyses were implemented in order to determine the chemical composition of these phases. The XRD spectra of the specimen 2 were examined (Fig 10), revealing that the microstructure composed of retained austenite, Cr_7C_3, Cr_3C_2 and FeC, carbides in the martensite matrix.

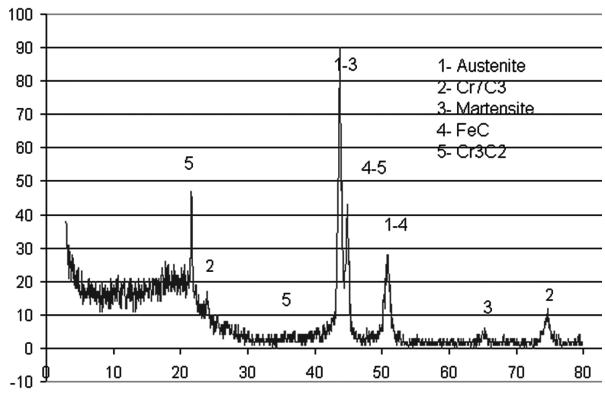

Fig. 10. X-ray diffraction spectrum taken from specimen alloyed with FeTi powders (pure argon+3% H_2 gas)

EDS analyses were performed on samples from the dendrites and intradentritic area on the coating of specimen 2 (see

Fig. 3). Of the (black) area marked with ''a" on the photograph, 89.45% consisted of Fe, 8.85% of Cr, 0.36 of Si and 1.34% of C (see Fig. 11a), while of the (white) area marked with ''b", 59.21% was composed of Fe, 38.26% of Cr and 2.37% of C (see Fig. 11b).

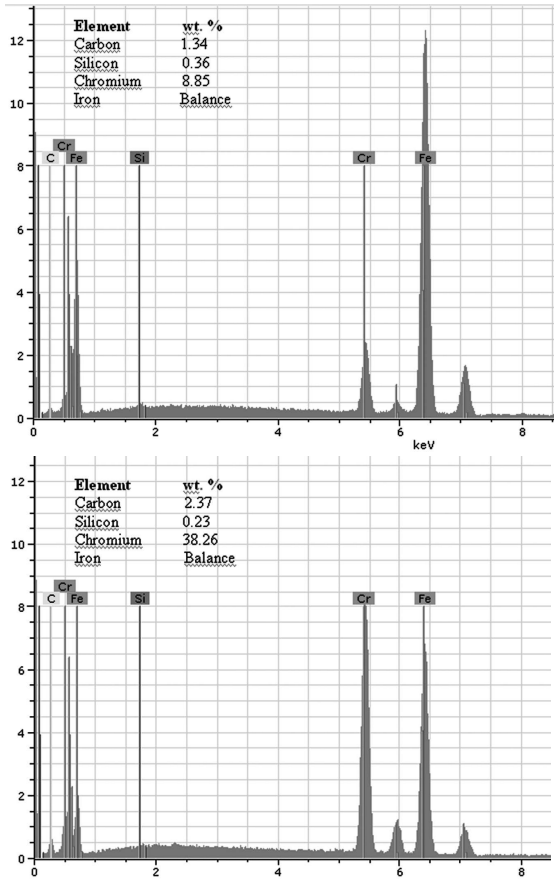

Fig. 11. a. EDS analysis of A point (89.45% Fe, 8.85% Cr, 0.36 Si and 1.34% C); b. EDS analysis of B point (59.21% Fe, 38.26% Cr and 2.37% C)

The XRD spectra of the specimen 5 (Fig 12) demonstrated that the microstructure consisted of carbides MoC, Fe_7C_3 and carbides in the ferro-molybdenum solid solution matrix. As sufficient energy input was formed in the welding bath due to the shielding hydrogen gas, some of the carbon atoms combined with Mo element and were formed on grain boundaries, while the rest combined with Fe element (see Fig. 5).

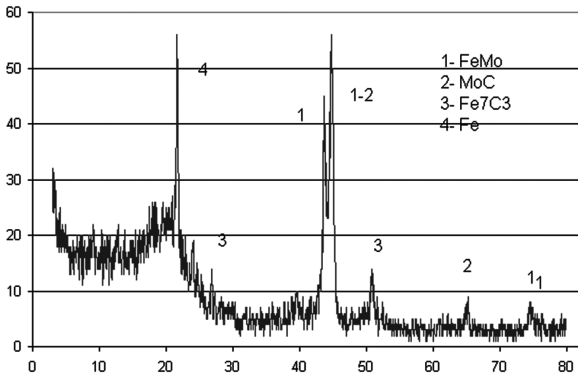

Fig. 12. X-ray diffraction spectrum taken from specimen alloyed with FeTi solid solution powders (pure argon+3% H_2 gas)

The chemical composition of the phases formed in the grain boundry (see Fig. 5), showed that this area contained 2.77% C, 38,69% Fe and 58.54% Mo (see Fig 13). An examination of the XRD spectra from the coating of specimen 9 revealed that the microstructure was composed of Fe_3C and TiC carbides in ferrit matrix (Fig 14).

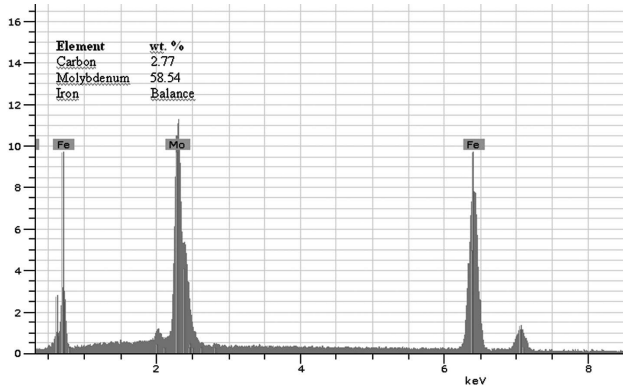

Fig. 13. EDS analysis of grain boundry (2.77% C, 38,69% Fe and 58.54% Mo)

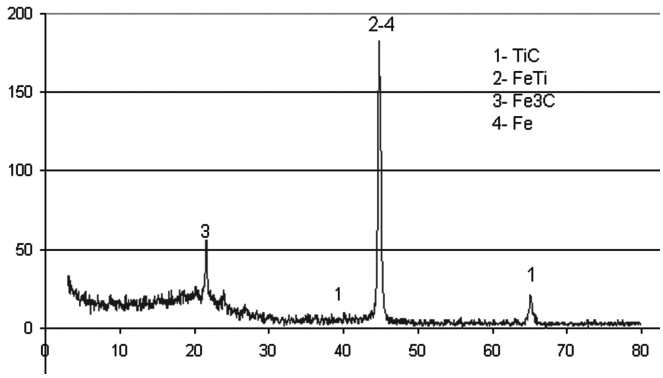

Fig. 14. X-ray diffraction spectrum taken from specimen alloyed with FeTi solid solution powders (pure argon+5% H_2 gas)

An analysis was performed on the matrix area marked with "a" on specimen 9 (see Fig. 15a), the results of which showed that the area contained 94.53% Fe, 3.79% Ti and 1.67% C, while the results from the band area marked with "b" (see Fig. 15b) revealed that it contained 39.56% Fe, 54.02% Ti and 2.73% C.

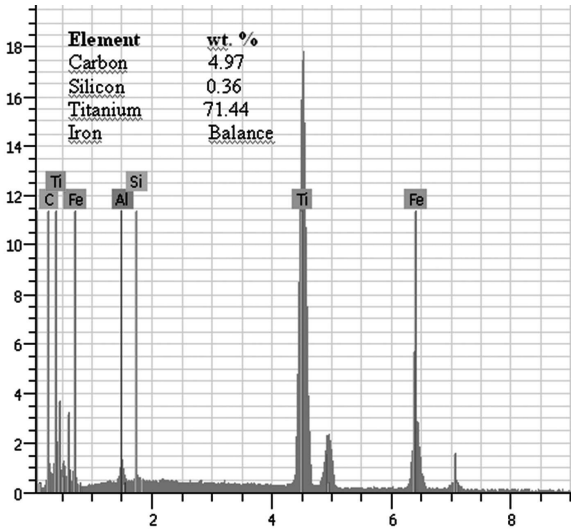

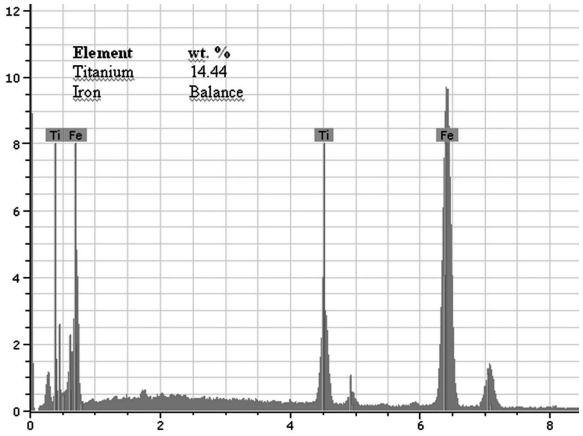

Fig. 15. a. EDS analysis of a point (94.53% Fe, 3.79% Ti and 1.67% C); b. EDS analysis of b point (39.56% Fe, 54.02% Ti and 2.73% C)

3.2. Hardness measurement

Volume hardness values of the coating layers of the samples which were exposed to surface modification are given in Table 3. The highest hardness was observed in the Specimen 1 among the samples which were exposed to FeCr powders. As explained in the microstructure section, rapid cooling occurring in the sample due to low energy input causes formation of the martensite phase which is hard and resistant. Although the hardness values of specimens 2 and 3 vary, this difference is not very high. Microstructures of the samples emerged in the Fe solid melt as a homogeneous and fine textured dendrite which contains M_7C_3 eutectic hard carbides. Dendrite sizes of the specimen 3 emerged larger. Because hydrogen addition into the shielding media causes excessive heat input. This can be attributed to the fact that hydrogen makes the arc more conductive to conduct heat during welding. A high amount of heat input leads to a lower hardness because of longer cooling time obtained in PTA welding in different shielding gas composition.

When the hardness values of specimens 4-6 which are exposed to surface alloying operation by using FeMo powders are compared, it was found that the specimen 5 has the highest hardness value. Coaxial, fine grained homogeneous matrix of the sample is covered with MoC phase in the grain boundary. In the specimen 4 in the same group, since not enough heat input was provided in the welding pool, the hardness of the ferro-molybdenum solid solution emerging with rough grains was lower. In the specimen 6, it is thought that gaps emerged due to the increasing rate of H_2 in the schielding gas, and this affected the hardness.

When the hardness values of the specimens 7-9 which were exposed to surface alloying operation by using FeTi powders are compared, the highest hardness value was found in the specimen 8. TiC carbides, emerging as homogeneous and fine-grained in the matrix due to adequate heat input increased the hardness value of the sample. In the specimen 7 in the same group, since the adequate amount of heat input of phase rich in element Ti could not be provided, it emerged as FeTi solid solution. In the specimen 9, it is thought that the pores occurred due to the increasing H_2 rate in the protective gas, and this affected hardness.

If all samples would be compared among each other, the highest hardness value would be seen in FeCr alloyed samples, and this is followed by FeMo and FeTi alloyed samples. If the hardness values based on protective gas mixture would be evaluated, P_3 in FeMo and FeTi alloyed samples affected the sample hardness values negatively. P_2 mixture gas affected homogeneous microstructure formation, therefore the hardness positively in all samples. P_3 mixture gas affected the hardness negatively in samples other than FeCr alloyed specimens.

3.3. Wear assessment

Figure 16 shows the graph representing the mass loss-load relationship of the specimens on which abrasive wear tests were performed after the surface alloying process.

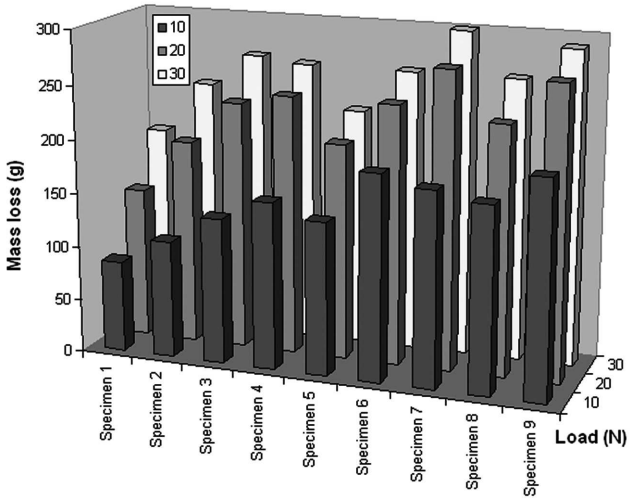

Fig. 16. Variation of mass loss with normal load for all specimens tested 80 mesh SiC

Amongst the arc-melted specimens (specimens 1-3), the lowest mass loss occurred in specimen 1. This lower mass loss in specimen 1 is directly related to the great amount of the martensite in the microstructure (see Fig. 2a-b). When examined specimen 2, the high wear resistance in this sample could firstly be attributed to its fine-grained microstructure. Moreover, Cr_7C_3, Cr_3C_2 carbides formed in dendrites and Fe_7C_3 carbides formed in Fe matrix also increased the sample's hardness and thus, its wear resistance. The increased mass loss in specimen 3 might be associated with its low surface hardness due to its coarsening microstructure.

An examination of the abrasive wear values of the samples surface-alloyed with FeMo shows that specimen 5 has a better wear resistance. This is due to the formation of a homogenous and fine-grained microstructure containing MoC and Fe_7C_3 carbides as a result of sufficient energy supply in the welding pool. Yet, no homogenous microstructure was formed in specimen 4 owing to insufficient energy supply. specimen 6 demonstrated the worst wear resistance among the FeMo alloyed samples, because as it can be seen in microstructure photo, the H_2 gaps emerging both in the grain limits and within the grains decreased the wear resistance of the sample.

A similar argument can also be made for the specimens surface-alloyed with FeTi. Among these specimens, the best wear resistance was again obtained in specimen 8, the sample

treated with surface alloying process in a shielding gas composition with an addition of 3% hydrogen. Adequate heat supply in the weld pool depending on the content of the shielding gas resulted in a homogeneous microstructure and formation of TiC particles in the microstructure. These rather hard particles formed in a soft matrix highly decreased the abrasive's cutting energy and energy of penetration into the matrix. Contrarily, the wear resistances of the samples exposed to processing in P_3 environment decreased substantially, because the increasing rate of H_2 in the protective gas created porosity in the microstructure between the matrix and TiC phase and decreased the strong adhesion of TiC phase to the matrix. Therefore, hard abrasive separated the TiC phase from the matrix with lower energy and caused more harm.

If the wear surfaces are analyzed in order to determine the wear mechanisms coming from the samples, it can be seen that the specimen 1 demonstrates an abrasion in type of microscratch and it has a smooth surface morphology due to the surface hardness it has (Fig. 17). It was seen in the specimen 2 that microscratch type abrasion (Fig. 18).

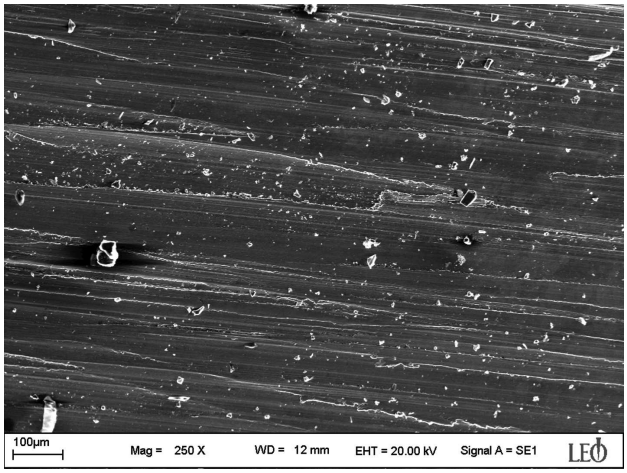

Fig. 17. Wear surface of the specimen 1 at 30 N load

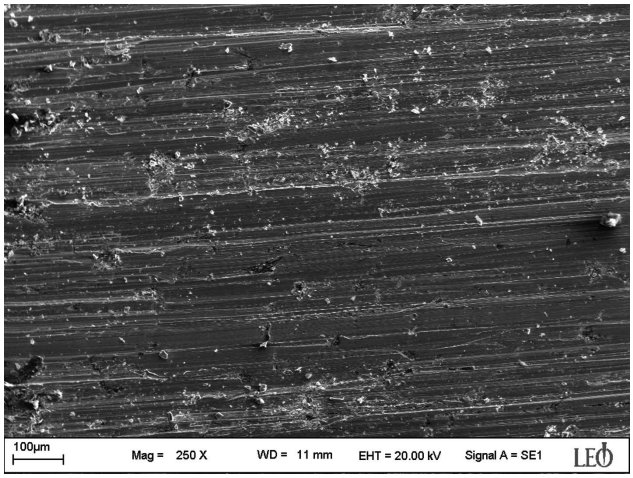

Fig. 18. Wear surface of the specimen 2 at 30 N load

It can be thought that this occurred because of tearing the hard eutectic carbides apart from the soft matrix. When the surface wear photographs of the specimen 6 which was subject to processing in P_3 composition is analyzed, it was found that the sample was exposed to extreme plastic deformation (Fig. 19). Micro scratch, local plastic deformation and micro abrasion was seen in specimen 9 (Fig. 20).

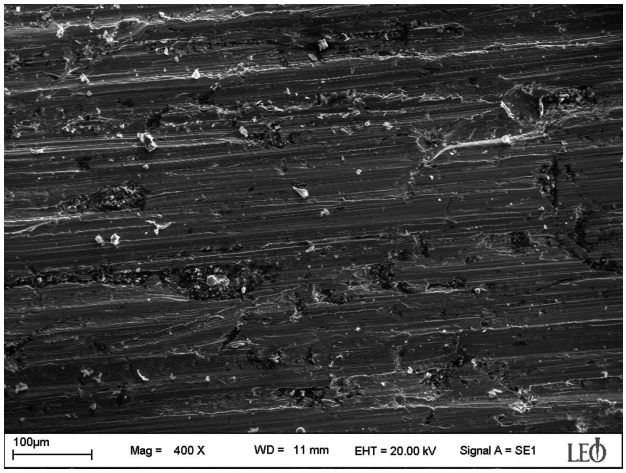

Fig. 19. Wear surface of the specimen 6 at 30 N load

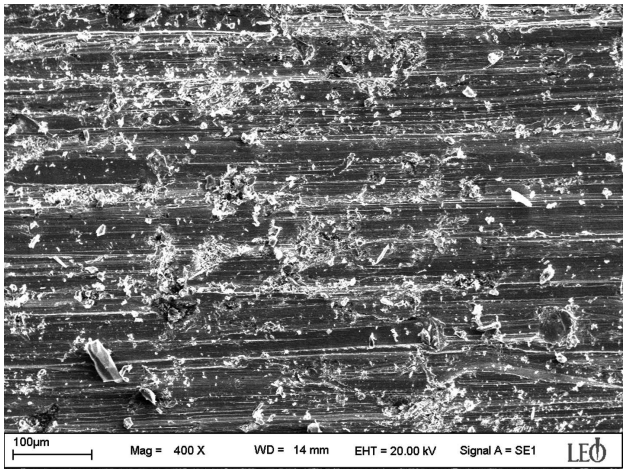

Fig. 20. Wear surface of the specimen 9 at 30 N load

In the occurring of deformation mechanism, the features of the material which is worn are also effective as well as the type, form of the abrasive and the force applied. The wear resistances of the fine and homogeneously distributed matrixes with high hardness are higher. The pores occurring both in the matrix and between the matrix and the second phase of the Fig. no. 6 and 9 decreased both hardness and the wear resistance of the samples. Moreover, the gaps between the phases caused heavy plastic deformation in the matrix during the detaching of the hard phase from the matrix.

4. Conclusions

Low-carbon steels were surface-alloyed with FeCr, FeMo and FeTi powders using the TIG welding method in two different shielding gas environments and the following results were obtained.

1. The changes in shielding gas composition affected the changes in the specimens' microstructures. The microstructure of the coating of the specimen alloyed with FeCr powders

was composed of Cr_7C_3, Fe_7C_3 carbides, while MoC, Fe_3C and FeC carbides were observed in the specimen alloyed with FeMo powders. The specimen with FeTi content consisted of TiC, Fe_3C phases.

2. The most homogenous microstructure and the highest wear resistance were obtained in the gaseous environment which included 3% of H_2. Increasing this rate to 5% in the protective gaseous environment caused gaps and pores in the microstructure and caused a decrease in the wear resistance

3. Among the specimens, the highest hardness value was obtained in the specimens alloyed with FeCr, followed by the specimens containing FeMo and FeTi. Among the specimens other than those alloyed with FeCr, surface hardness values were higher in the specimens treated in 3% H_2+ argon gas environment.

4. The lowest mass loss of wear was obtained from the surface of the specimen alloyed with FeCr powders and this was followed by the specimen with FeMo and FeTi.

5. The most homogeneous microstructure among all samples was obtained in P2 (Ar+3%H_2) protective gas mixture, and this was followed by P1 (pure Ar.). In the samples processed in P3 (Ar+5%H_2) environment, gaps and pores occurred.

REFERENCES

[1] A. Mazahery, M.O. Shabani, Archives Of Metallurgy And Materials **57**, 1 (2012).
[2] M. Gwozdzik, Z. Nitkiewicz, Archives Of Metallurgy And Materials **54**, 1 (2009).
[3] HM. Wang, CM. Wang, LX. Cai, Surf. Coat. Technol **168**, 202-208 (2003).
[4] L. Shepeleva, B. Medres, WD. Kaplan, M. Bamberger, A. Weisheit, Surf. Coat. Techno, 125, 45-48 (2000).
[5] HM. Wang, YF. Liu, Sci. Eng A **338**, 126-132 (2002).
[6] Y. Liu, J. Han, R. Li, W. Li, X. Xu, J. Wang, S. Yang, Applied Surface Science **252**, 7539-7544 (2006).
[7] R. Iakovou, L. Bourithis, G. Papadimitriou, Wear **252**, 1007-1015 (2002).
[8] QY. Hou, YZ. He, Q.A. Zhang, J.S. Gao, Materials & Design **28**, 1982-1987 (2007).
[9] RL. Deuis, JM. Yellup, C. Subramanian, Composites Science and Technology **58** (2), 299-309 (1998).
[10] C. Zhao, F. Tian, H. Peng, J. Hou, Surf. Coat. Technol **155**, 80-84 (2002).
[11] T. Hejwowski, Vacuum **83**, 166-170 (2008).
[12] S. Ozel, B. Kurt, I Somunkiran, N Orhan, Surface & Coatings Technology **202**, 3633-3637 (2008).
[13] J. Tusek, M. Suban, Int J Hydrogen Energy **25**, 369-376 (2000).
[14] M. Suban, J. Tusek, J Mater Process Technol **119**, 185-192 (2001).
[15] M. Suban, J. Tusek, Mater Process Technol **119**, 193-198 (2001).
[16] JJ. Lowke, R. Morrow, J. Haidar, AB. Murphy, IEEE Trans Plasma Sci. **25**, 925-30 (1997).
[17] B. Gülenç, K. Develi, N. Kahraman, A. Durgutlu, International Journal Of Hydrogen Energy **30**, 1475-1481 (2005).
[18] S. Mridha, Journal of Materials Processing Technology **168**, 471-477 (2005).
[19] MH. Korkut, MS. Gök, Tribology Materials, Surfaces & Interfaces **2**, 139-145 (2008).
[20] MH. Korkut, MS. Gök, Surface Engineering **25**, 517-525 (2009).
[21] VV. Cay, S. Ozan, MS. Gök, Journal of Coatings Technology and Research, in press.

Received: 10 April 2012.